Learning and Nonlinear Models - Journal of the Brazilian Society on Computational Intelligence (SBIC), Vol. 22, Iss. 2, pp. 30-47, 2024

DEEP LEARNING FOR SOLAR PANELS DEFECT CLASSIFICATION USING DATA AUGMENTATION STRATEGIES

Marcos Vinicius França Nunes
RAI - Robotics and Artificial Intelligence
Technologic and Exact Center
Federal University of Recôncavo da Bahia
Cruz das Almas, Brazil
marcosvinicius@aluno.ufrb.edu.br

André Luiz Carvalho Ottoni
Department of Computing
Federal University of Ouro Preto
Ouro Preto, Brazil
andre.ottoni@ufop.edu.br

Abstract – The inspection and maintenance of solar panels face significant challenges due to the dangers involved in checking for potential defects in photovoltaic panels. However, the advancement of studies to facilitate this verification is limited by the lack of image datasets for training algorithms that can perform this task. Based on this principle, the use of Convolutional Neural Networks (CNNs) for training and Data Augmentation for creating artificial data from real images is common. With that said, this work aims to explore configurations and models of Data Augmentation for the classification of defects in solar panels using CNNs. The proposed methodology consists of four experimental stages, where the application of Zoom, rotation, horizontal displacement, and vertical displacement transformations are evaluated, followed by filtering the best results and combining them to find the ideal classification model. The performance of the model proved to be most effective when using a 35-degree rotation for creating artificial images, thus achieving an 88% F1-Score and 87.64% accuracy.

Keywords – Machine learning, deep learning, data augmentation, convolutional neural networks, solar panels.

1 INTRODUCTION

The search for alternative energy sources is motivated by a potential scenario of natural resource scarcity, the increasing need for energy, and the worsening global climate situation [1]. In this regard, it is of paramount importance and urgency to popularize the use of renewable energies to reduce environmental deterioration. It becomes necessary for the global population to meet present needs without disrupting future demands. This is called sustainable development [2]. In this sense, photovoltaic energy is clean and contributes to environmental quality by not generating carbon emissions [3]. The work of [3] mentions several arguments that reinforce the advantages of preferring solar energy. Among these examples, the following stand out: the savings in water in reservoirs, which makes water less scarce for other uses, the reduction in investments in new hydroelectric plants, which could mean new investments in solar energy, and the creation of new jobs through the need for manufacturing and maintenance of solar panels.

It is important to mention the social and economic impacts that a change in the distribution of energy and how it is produced would entail. According to [2], the current model of centralized electricity production in large power plants, transporting electricity to major consumption centers via extensive transmission lines, results in urban areas being transformed into major population hubs. This consequently increases rural exodus, as these rural areas are often not provided with electricity. As a result, it becomes impossible to improve raw materials and rural work, leading workers to seek new opportunities in large cities. The development solution would be the decentralization of energy distribution as a substitute for fossil fuels. This would lead to the improvement of various rural areas, increasing the workforce and reducing social problems in cities. In a case study conducted by [4], it is presented that a significant investment is required for the installation of solar panels; however, in the long term, it proves to be a very good benefit. For residential installations, it was found that the solar energy system can pay for itself in 9 years, with an additional 16 years of significant profitability remaining. Solar energy is already being applied in agriculture for irrigation projects [5], in residential settings [4, 6, 7], in industry [8], in construction [9], in schools [1], among others.

Having a solar panel requires monitoring to check for the need for possible maintenance. Dust accumulation, temperature variations, and changes in irradiation affect the operation of solar panels [10]. These particles accumulate on any photovoltaic surface and can be defined as soiling [11]. The accumulation of dust reduces the amount of sunlight reaching the panel, resulting in lower energy production [10, 11], as well as causing a deviation in the angle of incidence of solar radiation [11]. The authors

of [12] compare two dirty panels and two clean panels from the manufacturer Solarex, model MSX56. The conclusion is that the clean panels showed an efficiency of 16.26% higher than the dirty panels. Another type of problem that can also occur with the panels due to climate changes and thus disrupt their operation is micro fissures, which can cause a drop in output power. Even with the microfissure, the panel continues to function, but its lifespan may be reduced [13]. To perform maintenance on photovoltaic panels, great care is necessary, especially for locations at great heights. For this reason, the use of a machine learning system is of paramount importance, in the sense of conducting inspections using drones, for example. This approach prevents individuals from climbing onto roofs, where there is a risk of falls and serious fractures, and also ensures that the maintenance professional is prepared for what they will encounter on the solar panel, avoiding unnecessary travel. Additionally, the use of deep learning for this task is important for operational efficiency, accuracy in identifying issues present on the panels, and minimizing downtime. The use of machine learning ensures the sustainable success of solar systems.

Several studies have already been conducted using deep learning applied to photovoltaic panels. In their work, [14] developed a classification system to detect anomalies such as partial shading and heating in photovoltaic panels using thermal images. They employed a method based on artificial neural networks, achieving an accuracy of 97% for multilayer perceptrons (MLP) and 87.5% for ABNET and PSOM networks. In this experiment, Artificial Neural Networks were used with the computational tool MATLAB and a small dataset of 120 thermographic images, which limits the system to only this type of image, also limiting the generalization of the results. Additionally, the images underwent preprocessing before being trained by the Neural Network. The research could be improved by including a wider range of potential defects and requiring a larger dataset for better reliability of the results. An approach using electroluminescence images is conducted by [15], where they employ a convolutional neural network (CNN). They achieve an average accuracy of 88.42% with CNNs and an average accuracy of 82.44% with support vector machines (SVMs). The authors implemented a hybrid system that involved several preprocessing steps, including electroluminescence image segmentation. The approach demonstrated that, although the CNN is computationally more expensive and suitable for environments with GPU capacity, it can offer significantly higher accuracy compared to SVMs. However, this requires a substantial amount of computational resources to train and run the CNN, making it an obstacle for environments with limited GPU capacity. The work of [16] proposes a technique for monitoring and detecting damages in solar panels and wind turbine blades. Images were captured by a high-resolution drone, and Data Augmentation techniques and deep neural networks were used to achieve accuracy rates higher than 97%. The captured images were preprocessed to remove noise and enhance image quality, making them suitable for analysis. Additionally, the model was trained with a dataset of labeled images to identify defects in solar panels and wind turbine blades. The training involved dividing the images into patches and using transformers to process these divisions as sequences of tokens. The major limitation encountered is the system dependence on high-quality data. Some images with low resolution and noise can affect the accuracy of defect detection. Additionally, for different types of defects and varied environmental conditions, its generalization may require further adjustments.

Recent studies have explored the use of CNNs for analyzing images captured by unmanned aerial vehicles (UAVs) in the inspection of solar panels. For example, the paper [17] presents in their review the work of [18], which proposes a CNN model using RGB images to detect defects in photovoltaic modules. The study showed good results but lacks a more detailed discussion on the CNN training process. Aspects such as the choice of initial hyperparameters, network structure, the number of filters used, and the adopted training approach were not comprehensively addressed. These details are crucial to evaluate the effectiveness and robustness of the proposed model. The authors of [19] review various works related to the application of neural networks in problems involving solar panels. Among all the cited works, the one by [20] stands out, presenting an innovative model called DeepSolarEye, a CNN designed to provide detailed information on dirt and defects in solar panels. DeepSolarEye not only predicts power loss caused by dirt but also locates the affected areas on the solar panels and categorizes the type of dirt. This approach is particularly notable for using weakly supervised learning, eliminating the need for labeled data to locate dirt during training. However, the DeepSolarEye model has some limitations. For instance, the approach relies on a significant amount of environmental data, such as solar irradiance and timing, which may not be readily available in all solar panel installations.

A good technique to increase the reliability of a classification system is the use of data augmentation [21, 22]. This technique is particularly recommended for databases with few images or those that are unbalanced, as it will increase the number of images, thus improving the dataset for neural network training. Having as much data as possible is crucial for better training of a Deep Learning system [21, 23, 24]. The concept of Data Augmentation is simply a set of algorithms that create synthetic data from the available dataset while preserving the labels. This process involves transforming the training dataset to better simulate real-world data [25]. Following this approach, the method aims to prevent overfitting [26, 27]. Overfitting occurs when the model does not generalize well to unseen data compared to observed data, which can lead to poor performance on the test set [28], thus compromising the model reliability. In this work, one of the objectives of using data augmentation is to avoid this problem. In the literature, the use of Deep Learning and Data Augmentation applied to solar panels is observed in the work of [29], which uses 10º rotation, 10% translation, and 0.2 radians of shearing. The authors of [30] made several DA modifications such as zoom, shift, blur, inversion, rotations, cropping, and resizing. At the end of their work, they concluded that the combination of shift and inversion yields the best results. It is shown by [31] that the types of transformations these newly created data undergo are geometric, such as position change, orientation, inversion, cropping, scaling, and rotation, as well as photometric transformations such as changes in color channels or lighting adjustments. The use of DA is mainly beneficial for small or unbalanced databases.

The authors of [23] conducted a study demonstrating the effectiveness of data augmentation in image classification, and some of their examples show better accuracy results when data augmentation is used. A notable example of classification compared dogs and goldfish, showing a 6% improvement (91.5% vs. 85.5%) when using DA. In the work of [24], an analysis was conducted using DA to enhance the detection of guardrail and skirting systems in construction sites. Geometric transformations (zoom,

shear, and rotation) were applied, and the results show a significant contribution to the model performance improvement. Among all the results, it is important to highlight the substantial improvement in accuracy during the testing phase. Precision results of 96.83%, 95.31%, and 85.92% were obtained for shear, rotation, and zoom transformations, respectively, compared to 77.92% for the original images, i.e., without DA modifications. Therefore, in this article, four different types of transformations were explored, namely: zoom, rotation, and vertical and horizontal displacements.

The main objective of this work is to explore configurations and models of Data Augmentation for the classification of defects in solar panels using CNNs. In parallel to this, it aims to improve the effectiveness of solar panel inspection methods, contributing to the optimization of the efficiency and durability of photovoltaic systems.

As main contributions of this work are:

- Development and implementation of a defect classification model for solar panels using four different transformations on the images. These transformations include Rotation, Zoom, Vertical Displacement, and Horizontal Displacement. Each of these techniques was chosen to increase the variability of the training data and improve the ability of the model to generalize to new images;
- Conducting an extensive battery of tests and experiments to ensure the reliability and robustness of the obtained results. This rigorous evaluation approach allowed for verifying the effectiveness of the model under various conditions and scenarios, providing valuable insights into its performance.

The present article is organized into five sections. Section 2 presents the step-by-step methodology followed for the realization of this article. Sections 3 and 4 present the results and comparisons with other works, respectively. Finally, Section 5 presents the conclusions and proposals for improvements in this work.

2 METHODOLOGY

This section presents the proposal for conducting this paper. Thus, it is structured as follows: (1) Dataset, (2) Neural architecture and hyperparameters , (3) Data Augmentation transformations, and (4) Design of experiments.

2.1 DATASET

The database used in this work comprises the combination of images from two datasets provided on the Kaggle platform [32, 33] with some modifications to the images such as cropping, for example, and the exclusion of duplicate images between the two datasets. Thus, at the end of the image preprocessing, a dataset with 3048 images remained. Of these, 1623 images are of defective boards, divided into 417 for testing and 1206 for training, and 1425 images are of clean boards, divided into 356 for testing and 1069 for training. The dataset is divided into two classes:

- Class 0: Defective boards;
- Class 1: Clean boards.

In class 0, boards with physical defects as well as dirty ones were found. Examples of the images are presented in Figures 2 and 3.

Figure 1: Example of class 1 image: clean board. Source: [32].

Figure 2: Example of class 0 image: defective boards. Source: [33].

2.2 NEURAL ARCHITECTURE AND HYPERPARAMETERS

In this work, the Convolutional Neural Network ResNet50 [34, 35] was utilized, loading it is pre-trained weights from ImageNet for image classification tasks. The model has 23,587,712 parameters and 50 layers. The images were of resolution 256x256 and had 3 color channels. The key idea of ResNet is its construction with residual blocks. These blocks undergo a series of convolutions, enabling the network to learn the differences between representations in deeper layers. This addresses the issue of performance degradation in neural networks [36]. The choice of ResNet is justified by its widespread usage in the literature [37, 38]. In this regard, the model import was performed using the Keras library, utilizing pre-trained weights from ImageNet, which is a large dataset. Therefore, this usage proves highly effective as these weights capture useful patterns that can be applied to a wide range of problems.

The definition of hyperparameters is of paramount importance for a CNN because it determines how it will operate and adapt to the model during training. These configurations are essential for the success of neural network training. Table 1 presents the hyperparameters used in this work.

Hyperparameter	
Epochs (Stages 1 and 2)	30
Epochs (Stage 3)	70
Learning rate	0.0001
Optimizer	Adam

Table 1: Hyperparameters.

2.3 DATA AUGMENTATION TRANSFORMATIONS

Four types of Data Augmentation transformations were chosen to generate new artificial images: Zoom, Rotation, Horizontal Shift (HS), and Vertical Shift (VS) using the image generator for Data Augmentation called ImageDataGenerator (IDG) from the Keras library (version 2.15.0). Figure 4 shows an example of an original dataset image, followed by a brief explanation of each modification performed, along with an example of each transformation applied.

Figure 3: Image of a solar panel without modifications.
Source: `https://www.kaggle.com/datasets/pythonafroz/solar-panel-images`

- Zoom: Ten floating-point values were chosen. When a value is selected, the new images are modified by decreasing or increasing their zoom. For example, when choosing a value of 0.67, the image will either gain 67% zoom or lose the same amount. In this experiment, the values chosen were 0.2, 0.4, 0.6, 0.8, 1.0, 1.2, 1.4, 1.6, 1.8, and 2.0. Figures 5 and 6 show examples of images with the application of zoom.

Figure 4: Image subtracted Zoom of 80%.

Figure 5: Image added Zoom of 80%.

- Rotation: For rotation, ten values in degrees were also chosen for the image to rotate randomly to the left or right, meaning that when selecting a value such as 30, the images can be rotated by 30 or -30 degrees. The chosen rotation values were 5º, 10º, 15º, 20º, 25º, 30º, 35º, 40º, 45º, and 50º. Figures 7 and 8 show images rotated to the right and the left.

Figure 6: Image rotated 45º to the right.

Figure 7: Image rotated 20º to the left.

- Horizontal Shift: In this transformation, the image is shifted horizontally, potentially to either side. For example, when selecting a value of 0.25, 25% of the image will be shifted to the left or right. In this item, five values were chosen: 0.2, 0.4, 0.6, 0.8, and 1.0. Figure 9 shows an image shifted to the right, and Figure 10 shows an image shifted to the left.

Figure 8: Image shifted 60% to the right.

Figure 9: Image shifted 60% to the left.

- Vertical Shift: Analogously to Horizontal Shift, this time the image is shifted vertically, meaning that when a certain value is chosen, the image will be shifted up or down. The chosen values were the same as for Horizontal Shift. Figure 11 shows an image shifted upwards, and Figure 12 shows an image shifted downwards.

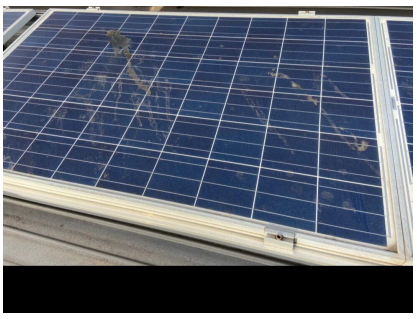

Figure 10: Image shifted 40% upwards.

Figure 11: Image shifted 40% downwards.

2.4 DESIGN OF EXPERIMENTS

The design of experiments aimed to conduct tests with the application of individual and combined Data Augmentation transformations, to select the best configurations at each stage. At the end of each training, accuracy, precision, recall, confusion matrix, and F1-Score results are generated on the test set of the experiment. The class of defective plates was defined as positive and clean plates as negative.

When training is performed, true positive (TP), true negative (TN), false positive (FP), and false negative (FN) values are generated [39]. These metrics are typically presented in a confusion matrix and have the following meanings:

- TP: number of images correctly classified as positive;
- TN: number of images correctly classified as negative;
- FP: number of images incorrectly classified as positive;
- FN: number of images incorrectly classified as negative.

These values are adopted for the calculations of the following metrics: accuracy, precision, recall and F1-Score. Accuracy is used to measure the proportion of correct predictions relative to the total predictions [39]. It is useful for getting an overall view of the model, but it is not the focus of this work as it is not the appropriate metric for imbalanced datasets. The calculation of accuracy is presented in Equation (1):

$$accuracy = \frac{TP + TN}{TP + TN + FP + FN}. \tag{1}$$

Precision measures the potential of the model to not classify a negative class as positive [39]. Thus, it shows how much one can trust the model when it says an image is of a certain class. Equation (2) presents the calculation of precision:

$$precision = \frac{TP}{TP + FP}. \tag{2}$$

Recall demonstrates the ability of the classifier to find all positive samples.[39], demonstrated by Equation (3):

$$recall = \frac{TP}{TP + FN}. \tag{3}$$

The F1-score is the harmonic mean between precision and recall, as shown in Equation (4) [39]. It demonstrates a significant balance between these two metrics and is also very useful when working with imbalanced datasets. For these reasons, the focus of the study on the results of this work is this metric.

$$F1\text{-}Score = \frac{2 \times \text{precision} \times \text{Recall}}{\text{precision} + \text{Recall}}. \tag{4}$$

In the next subsections, the three stages of this experiment are described in detail.

2.4.1 EXPERIMENTS WITHOUT DATA AUGMENTATION

At the beginning of the experiments, trials were conducted without the use of Data Augmentation, following the same format as the subsequent tests. The first experiment was analogous to the experiment codes of the 1st and 2nd stages, with 30 epochs. The second experiment extended to 70 epochs, the same quantity as the tests in the 3rd stage.

2.4.2 EXPERIMENTS OF STAGE 1: ANALYSIS OF INDIVIDUAL DATA AUGMENTATION TRANSFORMATIONS

In the first stage of the experiment, tests were conducted with each Data Augmentation transformation mentioned earlier. All selected values were experimented with and studied one by one to find the top 2 models of each type of modification to be used in the second stage. In total, 30 simulations were conducted in this first stage, each with 30 epochs, forming the four groups described in Table 2.

Transformation	Number of Experiments
Zoom	10
Rotation	10
Horizontal Shift	5
Vertical Shift	5
Total	30

Table 2: Experiments carried out in the 1st Stage.

The F1-Score metric was the priority in selecting the values that proceeded to the second stage. When equal values were encountered, the decision on which modification to choose was based on the test that exhibited better accuracy.

2.4.3 EXPERIMENTS OF STAGE 2: ANALYSIS OF DATA AUGMENTATION COMBINATIONS

In this stage, six groups were formed, each consisting of 4 tests. This allowed for testing all possible combinations between the best results from Stage 1, resulting in a total of 24 tests, each with 30 epochs. The six groups are outlined in Table 3.

Data Augmentation Combination
Zoom + Rotation
Zoom + Horizontal Shift
Zoom + Vertical Shift
Rotation + Horizontal Shift
Rotation + Vertical Shift
Horizontal Shift + Vertical Shift

Table 3: Data Augmentation Combinations of the 2nd Stage.

The top 2 results from each group would proceed to the third stage of experiments.

2.4.4 EXPERIMENTS OF STAGE 3: ANALYSIS OF THE BEST DATA AUGMENTATION COMBINATIONS

The third stage consisted of only one group with all the best experiments from Stage 2 combined. Additionally, this phase also involved an increase in the number of epochs from 30 in the first two stages to 70 in this third stage, aiming to have greater confidence in the results. This single group combined Zoom, Rotation, Horizontal Shift, and Vertical Shift, generating six combinations.

3 RESULTS

This section presents the main results of this work obtained from the experiments, highlighting the importance of using Data Augmentation. The section follows the following structure: (1) results from the stage without Data Augmentation, (2) results from stage 1, (3) results from stage 2, and (4) results from stage 3.

3.1 RESULTS FROM THE STAGE WITHOUT DATA AUGMENTATION

The initial experiments consisted of conducting tests without Data Augmentation, following the same format as the experiments with Data Augmentation, with 30 epochs similar to the first two stages and with 70 epochs, similar to the third, as shown in Table 4. These results will be used as a reference for the subsequent stages.

Epochs	Accuracy (%)	F1-Score (%)	Recall (%)	Precision (%)
30	83.05	83.00	83.00	83.00
70	83.31	83.00	83.00	83.00

Table 4: Results from the experiment without Data Augmentation.

3.2 RESULTS FROM STAGE 1: INDIVIDUAL DATA AUGMENTATION TRANSFORMATIONS

This section presents the results of the first stage of experiments with Data Augmentation. As described in the methodology, in this phase, the effects of individual Data Augmentation transformations were analyzed, and simulations were conducted with 30 epochs.

The Zoom tests are presented in Table 4. For the first two experiments of Data Augmentation with Zoom at 0.2 and also at 0.4, there is a tie in the F1-Score metric of 87.00%. Additionally, Zoom at 0.2 achieved 87.12% accuracy, 88.00% recall, and 87.00% precision. For Zoom at 0.4, the result was the same, with the difference in recall, which was 87,00%. Furthermore, with Zoom at 1.4, only 82.00% F1-Score was achieved, which presented the worst result in this test group. Analyzing a value closer to the best, with Zoom at 0.6, a decrease of 2.00% in F1-Score and 2.57% in accuracy can already be observed, as shown in Table 5. The top 2 values, 0.2 and 0.4, will undergo further testing in the second stage. Figure 13 presents all the results of the Zoom tests. It is noticeable that large Zoom values are not necessary to achieve good results because, higher Zoom values, the accuracy drops.

Zoom	Accuracy (%)	F1-Score (%)	Recall (%)	Precision (%)
0.2	**87.12**	**87.00**	**88.00**	**87.00**
0.4	**87.12**	**87.00**	87.00	**87.00**
0.6	84.55	85.00	85.00	86.00
0.8	84.94	85.00	86.00	86.00
1.0	84.17	84.00	85.00	86.00
1.2	85.58	86.00	86.00	86.00
1.4	82.36	82.00	83.00	86.00
1.6	83.14	83.00	84.00	84.00
1.8	84.16	84.00	84.00	84.00
2.0	83.27	83.00	84.00	85.00

Table 5: Results of Zoom in the 1st Stage.

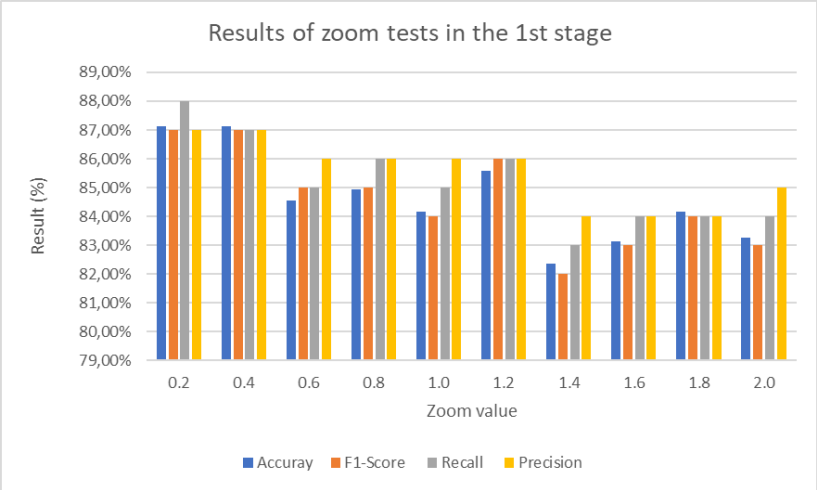

Figure 12: Results Graph of Zoom transformation (1st Stage).

The Rotation experiment is where the best results of this work lie. Overall, a good performance of above 85.00% F1-Score was achieved in 50.00% of the tests. Notably, the 35° rotation obtained 88.00% F1-Score, recall, and precision, along with 87.64% accuracy. Another notable result is from the 40° experiment, which shows the same values for F1-score, recall, and precision as the 35° transformation but with an accuracy of 87.51%, as shown in Table 6. In the case of Rotation, the 35° and 40° values will proceed to the next stage of the experiment, where they will undergo further transformations. Figure 14 presents a graph with all the results of the Rotation group experiments, showing a large number of high results close to the best.

Rotation(°)	Accuracy (%)	F1-Score (%)	Recall (%)	Precision (%)
5	86.61	87.00	87.00	87.00
10	84.04	84.00	85.00	86.00
15	85.58	86.00	87.00	87.00
20	86.61	87.00	87.00	87.00
25	86.87	87.00	87.00	87.00
30	85.84	86.00	87.00	87.00
35	**87.64**	**88.00**	**88.00**	**88.00**
40	**87.51**	**88.00**	**88.00**	**88.00**
45	82.36	82.00	83.00	85.00
50	85.45	85.00	86.00	85.00

Table 6: Results of Rotation in the 1st Stage.

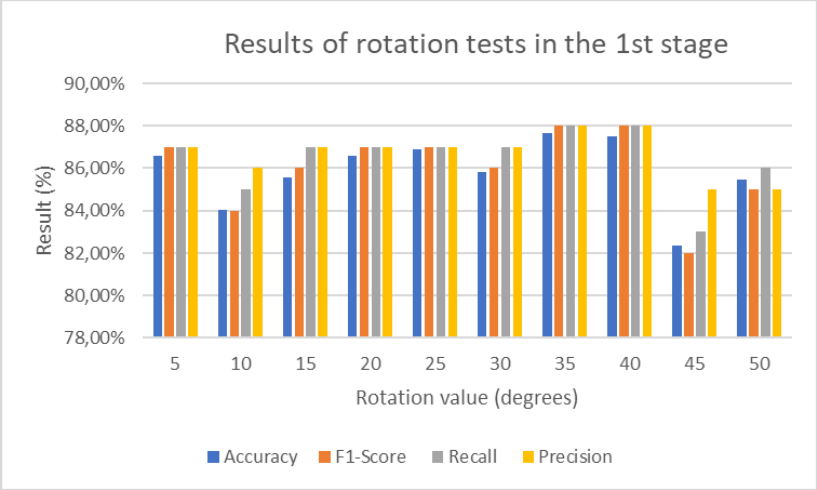

Figure 13: Results Graph of Rotation transformation (1st Stage).

The Horizontal Shift group showed good results in 60% of the conducted tests. Table 7 shows that the values of 0.4 and 0.6 stood out with 87% F1-Score and 88% precision each, with a difference of only 0.13% in accuracy. These two values differentiate themselves with better accuracy compared to 0.2 and 0.8 of Horizontal Shift, which obtained the same F1-Score value. The similarity between the first 4 tests is noticeable in Figure 15. Horizontal Shift at 1.0 appears to be ineffective for use in this scenario.

Horizontal Shift	Accuracy (%)	F1 - Score (%)	Recall (%)	Precision (%)
0.2	86,87	**87,00**	**87,00**	87,00
0.4	**87,38**	**87,00**	**88,00**	**88,00**
0.6	**87,25**	**87,00**	**88,00**	**88,00**
0.8	86,87	**87,00**	**88,00**	**88,00**
1.0	84,81	85,00	85,00	85,00

Table 7: Results of Horizontal Shift in the 1st Stage.

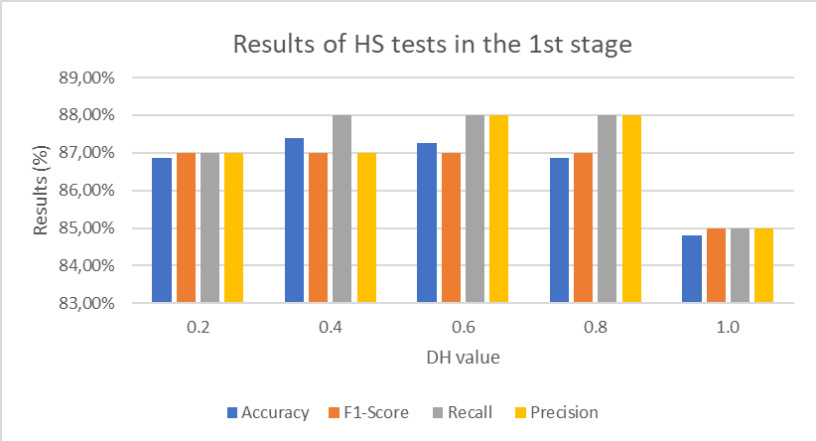

Figure 14: Results Graph of Horizontal Shift transformation (1st Stage).

The last test group in this first phase is with Vertical Shift. In this stage, most of the results above 85% were achieved, except for DV at 0.8, which showed an F1-Score of 84.00%. Therefore, the best results were obtained with 0.6, which showed 87.00% accuracy, F1-Score, Recall, and Precision, and also DV at 1.0, which shows 86.87% accuracy and 87% in the other metrics, as presented in Table 8, and all the results shown in Figure 16.

Vertical Shift	Accuracy (%)	F1 - Score (%)	Recall (%)	Precision (%)
0.2	85,45	85,00	85,00	85,00
0.4	86,46	86,00	**87,00**	86,00
0.6	**87,00**	**87,00**	**87,00**	**87,00**
0.8	84,16	84,00	84,00	84,00
1.0	**86,87**	**87,00**	**87,00**	**87,00**

Table 8: Results of Vertical Shift in the 1st Stage.

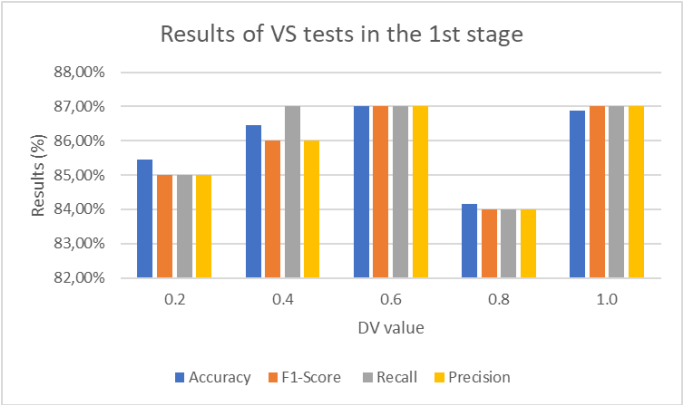

Figure 15: Results Graph of Vertical Shift transformation (1st Stage).

Therefore, the selected transformations for Stage 2 are presented in Table 9.

Transformation	Value	Accuracy (%)	F1-Score (%)	Recall (%)	Precision (%).
Zoom	0.2	87.12	87.00	88.00	87.00
Zoom	0.4	87.12	87.00	87.00	87.00
Rotation	35º	87.64	88.00	88.00	88.00
Rotation	40º	87.51	88.00	88.00	88.00
Horizontal Shift	0.4	87.38	87.00	88.00	88.00
Horizontal Shift	0.6	87.25	87.00	88.00	88.00
Vertical Shift	0.6	87.00	87.00	87.00	87.00
Vertical Shift	1.0	86.87	87.00	87.00	87.00

Table 9: Best results from Stage 1.

3.3 RESULTS OF STAGE 2: DATA AUGMENTATION COMBINATIONS

In this section, the results of the second phase of experiments with Data Augmentation are presented. For this purpose, simulations were carried out by combining the best transformations from the first Stage. Each of the 6 groups in this Stage contains 4 tests, thus generating 24 experiments.

The first group to stand out is the Zoom group, with 0.2 and 0.4 as the best values, combined with Rotation, which has 35º and 40º as the best results. Table 10 presents the best result of this Stage, which was the Data Augmentation transformation (Zoom (0.2), Rotation (35º)). This trial resulted in an F1-score of 84.00%, a Recall of 85.00%, and a Precision of 84.00%, a value below expectations considering that good values were obtained in the first Stage of tests. In the other experiments of this group, the system achieved an F1-Score of 84.00% in the combinations (Zoom (0.2), Rotation (40º)) and (Zoom (0.4), Rotation (35º)), with (Zoom (0.2), Rotation (35º)) being a better result due to its accuracy. Figure 17 presents all the results of this group, including the one considered worst, which was (Zoom (0.4), Rotation (40º)) with an F1-Score of 83.00%.

Zoom	Rotation (º)	Accuracy (%)	F1 - Score (%)	Recall (%)	Precision (%)
0.2	35	**84.34**	**84.00**	**85.00**	**84.00**
0.2	40	83.70	**84.00**	84.00	**84.00**
0.4	35	84.08	**84.00**	84.00	**84.00**
0.4	40	83.31	83.00	84.00	83.00

Table 10: Results of the combination of Zoom and Rotation in Stage 2.

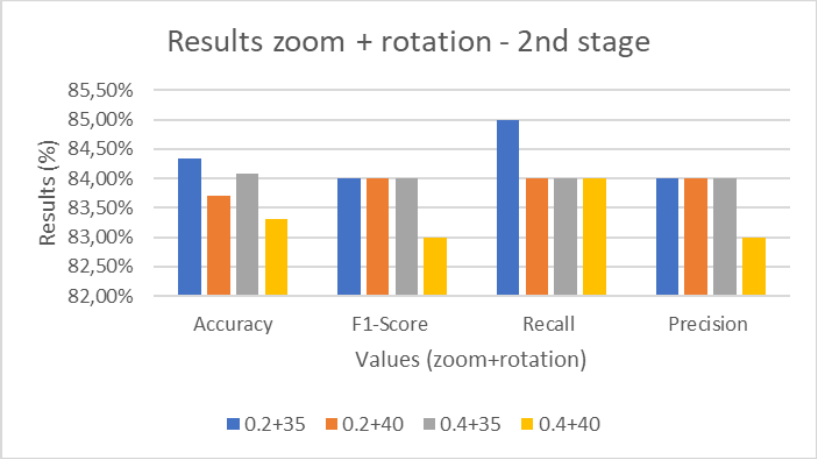

Figure 16: Results Graph of (Zoom + Rotation) combiation (2nd Stage).

The next test group is Zoom and Horizontal Shift. The best result of this test was also an 84.00% F1-score with the combination of (Zoom (0.4), HS (0.6)). Additionally, this test showed 84.08% accuracy, 84.00% precision, and 85.00% recall, as shown in Table 11. On the other hand, this combination only yielded one result below the standard, which was (Zoom (0.2), HS (0.6)), showing 81.00% F1-score and 80.85% accuracy. The other two results of (Zoom (0.2), HS (0.6)) and (Zoom (0.4), HS (0.4)) presented results close to those in Table 11, as observed in Figure 18.

Zoom	DH	Accuracy (%)	F1 - Score (%)	Recall (%)	Precision (%)
0.2	0.4	83.18	83.00	84.00	84.00
0.2	0.6	80.85	81.00	82.00	83.00
0.4	0.4	83.44	83.00	84.00	**85.00**
0.4	0.6	**84.08**	**84.00**	**85.00**	84.00

Table 11: Results of the combination of Zoom and Horizontal Shift in Stage 2.

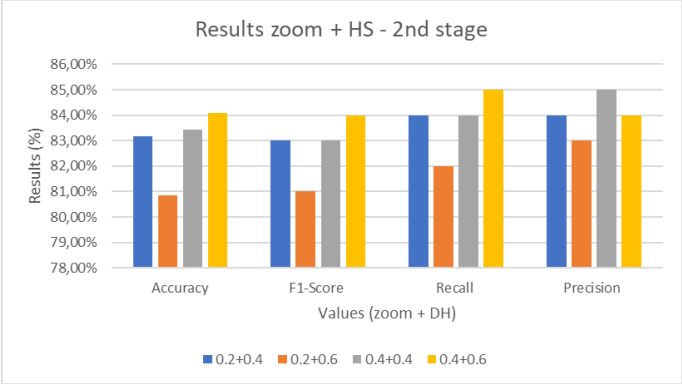

Figure 17: Results Graph of (Zoom + Horizontal Shift) combination (2nd Stage).

The last combination using Zoom is paired with the Vertical Shift transformation. In this part, we find the best value at the combination of 0.2 (Zoom (0.2), VS (1.0)), which achieved, like the previous ones, an 84.00% F1-score. Additionally, this experiment also showed 84.47% accuracy, 85.00% recall, and 84.00% precision, as presented in Table 12. As shown in Figure 19, two other combinations, (Zoom (0.2), VS (0.6)) and (Zoom (0.4), VS (0.6)), also achieved an 84.00% F1-score. The lowest value in this part was for (Zoom (0.4), VS (1.0)), which presented an 81.00% F1-score.

Zoom	VS	Accuracy (%)	F1 - Score (%)	Recall (%)	Precision (%)
0.2	0.6	84.06	**84.00**	**84.00**	84.00
0.2	1.0	**84.47**	**84.00**	**85.00**	84.00
0.4	0.6	84.08	**84.00**	**85.00**	**85.00**
0.4	1.0	80.60	81.00	82.00	84.00

Table 12: Results of the combination of Zoom and Vertical Shift in Stage 2.

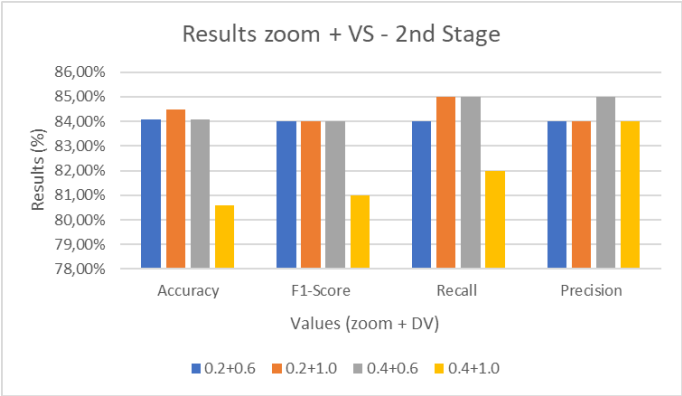

Figure 18: Results Graph of (Zoom + Vertical Shift) combination (2nd Stage).

In the sequence, another experiment involving rotations showed its best results with 35º and 40º. The first test with these values is with DH, which showed 0.4 and 0.6 as the best results. The highest performance of this trial came with (Rotation (35º), HS (0.4)), which also achieved the standard of this Stage of an 84.00% F1 score, along with the same value for the other metrics presented in Table 13. The other Data Augmentation transformations in this experiment obtained lower results in all aspects, as shown in Figure 20.

Rotation (º)	HS	Accuracy (%)	F1 - Score (%)	Recall (%)	Precision (%)
35	0.4	**84.34**	**84.00**	**84.00**	**84.00**
35	0.6	83.44	83.00	83.00	83.00
40	0.4	82.14	82.00	82.00	82.00
40	0.6	82.66	83.00	83.00	83.00

Table 13: Results of the combination of Rotation and Horizontal Shift in Stage 2.

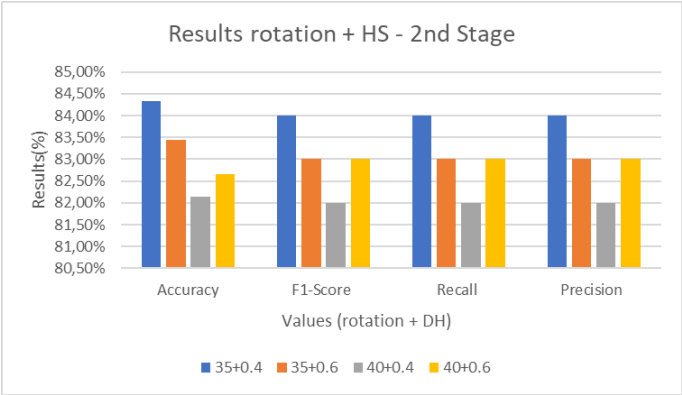

Figure 19: Results Graph of (Rotation + Horizontal Shift) combination (2nd Stage).

The last group involving Rotation in this Stage is its combination with the Vertical Displacement method. This test presents the best result as (Rotation (40º), VS (0.6)), thus showing an 84.00% F1-score and Recall, 83.82% accuracy, and 85.00% precision, values exposed in Table 14. This F1-score value is the highest in the group of experiments for this combination, which is evident in Figure 21.

Rotation (º)	VS	Accuracy (%)	F1 - Score (%)	Recall (%)	Precision (%)
35	0.6	83.18	83.00	83.00	83.00
35	1.0	83.18	83.00	83.00	83.00
40	0.6	**83.82**	**84.00**	**84.00**	**85.00**
40	1.0	82.92	83.00	83.00	83.00

Table 14: Results of the combination of Rotation and VS in Stage 2.

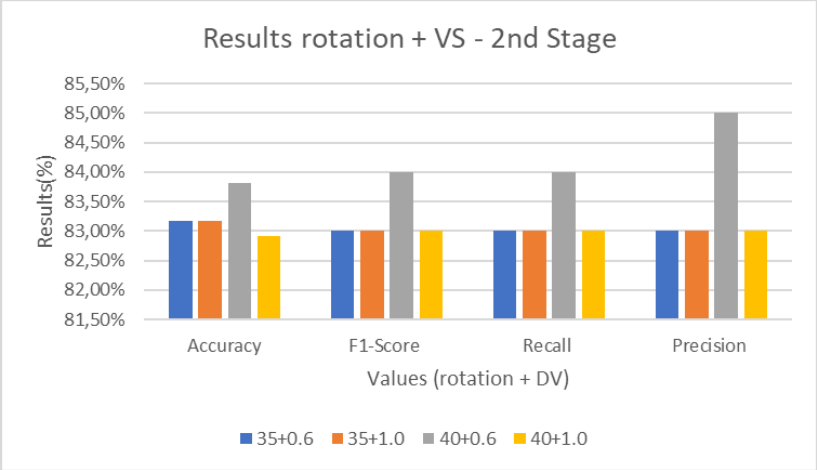

Figure 20: Results Graph of (Rotation + Vertical Shift) combination (2nd Stage).

In the last test of this Stage, the best results of this phase were obtained. For this reason, instead of choosing only one result to move to the third Stage, two were selected. These two results deviated from the standard of this Stage, as shown in Table 15. The combination of HS and HV had two standout results, combining 0.6 in both, achieving an 85.00% F1-score, Recall, and Precision, along with 85.25% accuracy. The Data Augmentation transformation (HS (0.6), VS (1.0)) exhibited the best result of the second Stage with an 86.00% F1-score, Recall, and Precision, along with 86.28% accuracy. Figure 22 shows that applying (HS (0.4), VS (0.6)) yields a good result of 85.00% F1-score. In this phase, only (HS (0.4), VS (1.0)) presented a value below the standard in this Stage.

HS	VS	Accuracy (%)	F1 - Score (%)	Recall (%)	Precision (%)
0.4	0.6	85.25	85.00	86.00	85.00
0.4	1.0	85.25	84.00	84.00	84.00
0.6	0.6	**85.25**	85.00	85.00	85.00
0.6	1.0	**86.28**	**86.00**	**86.00**	**86.00**

Table 15: Results of the combination of HS and VS in Stage 2.

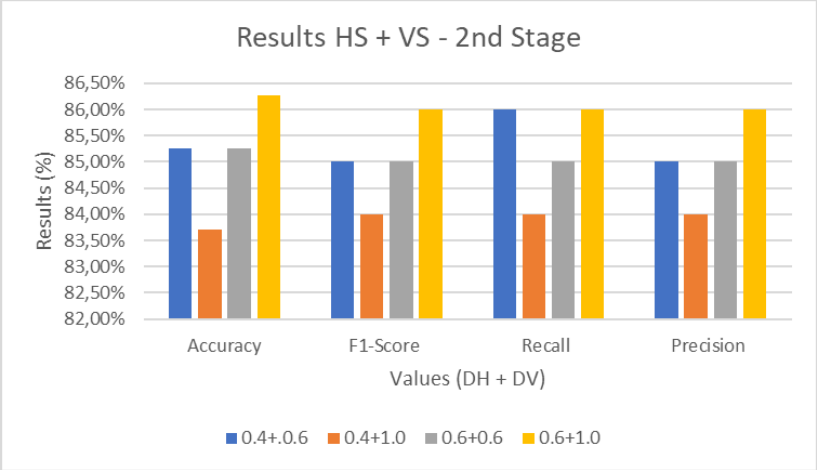

Figure 21: Results Graph of (Horizontal Shift + Vertical Shift) combination (2nd Stage).

3.4 RESULTS OF STAGE 3

Stage 3 comprised only one group formed by all modifications made to the images, totaling 6 tests with Zoom, Rotation, Horizontal Displacement, and Vertical Displacement. Table 16 presents all tests conducted in this Stage. The test with (Zoom (0.4), Rotation (35°), HS (0.6), VS (1.0)) yielded the best result with 85.00% in F1-score, Recall, and Precision, along with 84.60% accuracy.

Training did not perform well when the combination was (Zoom (0.2), Rotation (35°), HS (0.6), VS (0.6)). The result was 82.00% F1-score, the lowest value among all experiments.

Zoom	Rotation	HS	VS	Accuracy (%)	F1 - Score (%)	Recall (%)	Precision (%)
0.2	35º	0.4	0.6	84.34	84.00	84.00	84.00
0.4	35º	0.6	1.0	**84.60**	**85.00**	**85.00**	**85.00**
0.2	35º	0.6	0.6	82.40	82.00	83.00	84.00
0.2	35º	0.6	1.0	84.08	84.00	**85.00**	**85.00**
0.4	35º	0.6	1.0	84.22	84.00	**85.00**	84.00
0.4	35º	0.6	0.6	84.34	84.00	84.00	84.00

Table 16: Results of Stage 3.

3.5 RANKINGS OF THE BEST AND WORST DATA AUGMENTATION CONFIGURATIONS

Table 17 presents the ranking of the best configurations in the simulations. Additionally, the percentage difference of the Data Augmentation configuration compared to the reference experiment (without Data augmentation application) is evaluated.

Position	Data Augmentation Combination	Epochs	Accuracy (%)	Difference (%)
1)	Rotation (35º)	30	87.64	+ 4.59
2)	Rotation (40º)	30	87.51	+ 4.46
3)	HS (0.4)	30	87.38	+ 4.33
4)	HS (0.6)	30	87.25	+ 4.20
5)	Zoom (0.2)	30	87.12	+ 4.07
6)	Zoom (0.4)	30	87.12	+ 4.07
7)	VS (0.6)	30	87.00	+ 3.95
8)	Rotation (25º)	30	86.87	+ 3.82
9)	HS (0.2)	30	86.87	+ 3.82
10)	HS (0.8)	30	86.87	+ 3.82
Reference	Without Data Augmentation	30	83.05	–

Table 17: Top 10 rankings of Data Augmentation combinations in terms of accuracy

Table 18 presents the 10 worst results in this study. It is noticeable that even among the worst, two values were above the result from Table 2. The combination (Zoom (0.4), VS (1.0)) with 30 epochs achieved the worst results, which shows an accuracy of 80.60%. At this point, it is also important that eight configurations performed worse than without Data Augmentation, reinforcing the need to carefully adjust these transformations.

Position	Data Augmentation Combination	Epochs	Accuracy (%)	Difference (%)
1)	Zoom (0.4) + VS (1.0)	30	80,60	− 2,45
2)	Zoom (0.2) + HS (0.6)	30	80,85	− 2,20
3)	Rotation (40º) + HS (0.4)	30	82,14	− 0,91
4)	Zoom (1.4)	30	82,36	− 0,69
5)	Rotation (45º)	30	82,36	− 0,69
6)	Zoom (0.2) + Rotation (35º) + DH (0.6) + DV (0.6)	70	82,40	− 0,65
7)	Rotation (40º) + DH (0.6)	30	82,66	− 0,39
8)	Rotation (40º) + DV (1.0)	30	82,92	− 0,13
9)	Zoom (1.6)	30	83,14	+ 0,09
10)	Zoom (0.2) + DH (0.4)	30	83,18	+ 0,13
Reference	Without Data Augmentation	30	83,05	–

Table 18: Ranking of the 10 worst Data Augmentation combinations in terms of accuracy.

4 COMPARISON WITH OTHER WORKS

In this section, a comparison of this work with others that also use Deep Learning in the context of solar panels is presented. The compared works are [14], [18], [40], and [41]. Table 19 shows that most of the works are focused on defect detection. In contrast, this research focuses on the classification of defects in solar panels. A major contribution of this work is the use of different Data Augmentation hyperparameters for classification, thus expanding the range of possibilities in the study of Deep Learning applied to photovoltaic panels.

The authors of [40] used Data Augmentation to increase their data. The transformation adopted was Gaussian noise, which applies an effect aimed at reducing noise in the image and also creating some blurring in certain regions of the image. This application improved the accuracy of detecting smaller objects in the image. In contrast, this work used Zoom, Rotation, HS, and VS transformations to increase the image dataset for better system performance.

	Proposed	**[14]**	**[18]**	**[40]**	**[42]**
Deep Learning	✓	✓	✓	✓	✓
Classification	✓	·	✓	✓	·
Detection	·	✓	·	✓	✓
Transfer Learning	✓	·	✓	✓	·
Thermographic Images	·	✓	·	·	·
Images without photometric modifications	✓	·	✓	✓	✓
RGB images	✓	·	✓	✓	✓
Data Augmentation	✓	·	✓	✓	·
Accuracy $\geq 85\%$	✓	✓	✓	✓	✓

Table 19: Comparison of works.

Following the comparison, the ResNet architecture with transfer learning, as used in this work, was also found in the study by [40]. In addition to this architecture, the authors utilized Yolov3. Combining Yolov3 with ResNet with 101 layers can increase the computational complexity of the work, requiring greater hardware usage. The same happens in the work by [42]. The use of deep neural networks such as the Bidirectional Attention Feature Pyramid Network together with ResNet101 may require higher computational usage. In this proposed work, the computational complexity is lower due to the use of ResNet50, which has fewer layers, resulting in reduced memory usage and processing. This not only makes the method more efficient but also more accessible for implementation in systems with limited computational resources, without compromising the accuracy of anomaly classification.

The work of [14] proves to be quite useful for thermographic images; hence, the accuracy of detection can be affected by the camera quality and weather conditions at the time of image capture. Furthermore, the images need to undergo extensive preprocessing before being trained on the CNN, which can be labor-intensive and prone to errors. On the other hand, the proposed work uses RGB images, which are easier to obtain and less dependent on specific conditions. Additionally, the proposed method eliminates the need for extensive preprocessing, making the process more efficient and less error-prone. This simplified approach not only reduces time and costs but also enhances the robustness and practical applicability of anomaly classification.

The work by [18] presents excellent results in identifying various different types of defects in photovoltaic modules using a deep learning-based approach. However, a significant limitation of this method is that it relies on the presence of previously known and labeled defect types during training. If new types of defects that were not present in the training dataset emerge, the neural network may have difficulty correctly identifying them, potentially leading to a reduction in the effectiveness of the system.

In contrast, the system proposed in the present work adopts an innovative approach, focusing on learning the characteristics of a solar panel under optimal conditions. This method allows the system to identify anomalies with greater flexibility. Any deviation from the ideal state is detected as a potential defect, regardless of whether it is a known or unknown type of defect. This approach not only improves defect detection capabilities but also increases the system robustness and adaptability to new challenges and unforeseen conditions.

It is also worth highlighting that the present work, with the adopted CNN models and Data Augmentation, achieved an accuracy level of 87.64%. This level of accuracy ($\geq$ 85%) is also found in the compared works [14], [18], [40], and [42], indicating excellent models for classification and detection of defects in solar panels.

5 CONCLUSION

This work aimed to find the best model using Data Augmentation for the classification of defects in solar panels using CNNs. Thus, the current study focuses its contributions and results on: (i) the use of Deep Learning for defect classification in solar panels; (ii) the use of Data Augmentation for this purpose.

The results of this study are quite significant in the context of the photovoltaic industry. Accurate detection of defects plays an important role in maintaining the efficiency and safety of solar systems. Additionally, it can lead to a reduction in costs associated with monitoring these panels, thereby resulting in greater confidence in the distribution of solar systems. The accuracy of 87.64% and the F1-Score of 88% in the 1st Stage with a 35º Rotation demonstrate the potential of Deep Learning and Data Augmentation approaches to address this complex challenge. It is also important to highlight the results of Zoom at 0.2 and 0.4, where they presented an F1-Score of 87% and an accuracy of 87.12% each, thus showing that this Data Augmentation modification performs up to 4.59% better in accuracy when used alone and 5% more in F1-Score. It becomes evident that the top 10 results were in the first stage, where it was not necessary to use a large number of modifications and a high number of epochs. The best result with more than one modification is in the experiment of HS at 0.6 with VS at 1.0, which presented an accuracy of 86.28% with an F1-Score and Recall of 86%. For comparison, only 8 tests showed results below those found in tests without Data augmentation, the 10 worst results; there were still 2 tests with better results than without Data augmentation. Therefore, this study contributes to the literature by highlighting the effectiveness of the combined use of CNNs and Data Augmentation techniques in the classification of defects in solar panels.

In future work, we anticipate the use of other training models [14], the utilization of additional Data Augmentation methods for a broader range of transformations [24], and the exploration of other CNN architectures with transfer learning. Additionally,

applying further Data Augmentation transformations to achieve better performance in the CNN model and utilizing different datasets, such as drone images. In other datasets, like those captured by aerial cameras, it may be necessary to employ different data augmentation methods to attain satisfactory results, as the transformations used were particularly useful for this specific dataset. This distinction should be considered when applying data augmentation in different contexts. The use of Generative Adversarial Networks (GANs) to generate more datasets of solar panel images is a promising proposal for future projects, as demonstrated by [43]. This approach will allow for the acquisition of a significantly larger amount of material, enabling the conduct of new experiments with different neural architectures and the utilization of various optimizers. The generation of new synthetic data can help overcome limitations of real datasets, improve the robustness and generalization of models, and accelerate the development of innovative solutions in the field of solar energy.

ACKNOWLEDGMENTS: The authors are grateful to UFRB (Edital PROPAAE 005/2024) and UFOP (Edital PROPPI 18/2024).

REFERENCES

[1] N. H. G. S. da Silva and E. C. M. Araújo. "Desenvolvimento de projeto de para aproveito de energia solar numa escola pública de Brasília". *Programa de Iniciação Científica-PIC/UniCEUB-Relatórios de Pesquisa*, vol. 2, no. 1, 2016.

[2] R. A. Shayani, M. d. Oliveira and I. d. T. Camargo. "Comparação do custo entre energia solar fotovoltaica e fontes convencionais". In *Congresso Brasileiro de Planejamento Energético (V CBPE). Brasília*, p. 60, 2006.

[3] M. Bursztyn. "Energia solar e desenvolvimento sustentável no Semiárido: o desafio da integração de políticas públicas". *Estudos Avançados*, vol. 34, pp. 167–186, 2020.

[4] A. A. Palma and C. L. A. Lessa. "Implantação de placas fotovoltaicas em sistemas residenciais: estudo de caso". *RECIMA21-Revista Científica Multidisciplinar-ISSN 2675-6218*, vol. 3, no. 12, pp. e3122374–e3122374, 2022.

[5] A. C. Alvarenga, V. H. Ferreira and M. Z. Fortes. "Energia solar fotovoltaica: uma aplicação na irrigação da agricultura familiar". *Sinergia, São Paulo*, vol. 15, no. 4, pp. 311–318, 2014.

[6] F. M. COSTA *et al.*. "Utilização de painéis fotovoltaicos em residências". *Revista Diálogos: Economia e Sociedade (ISSN: 2594-4320)*, , no. 1, pp. 61–69, 2019.

[7] L. M. dos SANTOS and B. B. BLANCO. "Custo e benefício de painéis fotovoltaicos em residências no rio de janeiro". *Revista Tecnológica da Universidade Santa Úrsula*, vol. 5, no. 1, pp. 89–102, 2022.

[8] E. C. Coelho and G. S. Ronsani. "Utilização de Energia Solar nas Indústrias". *Revista de Ciências Exatas e Tecnologia*, vol. 14, no. 14, pp. 06–08, 2019.

[9] R. A. L. Roque and A. C. Pierri. "Uso inteligente de recursos naturais e sustentabilidade na construção civil". *Research, society and development*, vol. 8, no. 2, pp. e3482703–e3482703, 2019.

[10] A. G. Borbon. "Desenvolvimento de um sistema de inspeção de painéis solares autónomo baseado em técnicas de processamento de imagem e uso de UAVs". Ph.D. thesis, Universidade do Minho, 2024.

[11] C. A. C. Duarte. "O Impacto Do Soiling Nos Painéis Fotovoltaicos". Ph.D. thesis, Universidade de Lisboa, 2022.

[12] R. N. Michels, J. A. A. d. Santos, E. Gnoatto, M. Fischborn and E. Kavanagh. "Influência do acúmulo de poeira sobre a eficiência de paineis fotovoltaicos na região oeste paranaense". *Revista Agrogeoambiental*, vol. 1, no. 3, dez. 2009.

[13] M. H. V. d. Oliveira. "Impacto de microfissuras em módulos solares de silício em sistemas fotovoltaicos". Ph.D. thesis, Universidade de Caxias do Sul, 2021.

[14] R. H. F. Alves, G. A. de Deus Júnior, F. H. T. Vieira, M. S. de Castro, S. G. de Araújo and R. P. Lemos. "Detecçao de anomalias em painéis fotovoltaicos utilizando redes abnet, psom e mlp". In *Congresso Brasileiro de Energia Solar-CBENS*, pp. 1–8, 2016.

[15] S. Deitsch, V. Christlein, S. Berger, C. Buerhop-Lutz, A. Maier, F. Gallwitz and C. Riess. "Automatic classification of defective photovoltaic module cells in electroluminescence images". *Solar Energy*, vol. 185, pp. 455–468, 2019.

[16] D. Dwivedi, K. V. S. M. Babu, P. K. Yemula, P. Chakraborty and M. Pal. "Identification of surface defects on solar pv panels and wind turbine blades using attention based deep learning model". *Engineering Applications of Artificial Intelligence*, vol. 131, pp. 107836, 2024.

[17] T. Berghout, M. Benbouzid, X. Ma, S. Djurović and L.-H. Mouss. "Machine Learning for Photovoltaic Systems Condition Monitoring: A Review". In *IECON 2021 – 47th Annual Conference of the IEEE Industrial Electronics Society*, pp. 1–5, 2021.

[18] X. Li, Q. Yang, Z. Lou and W. Yan. "Deep learning based module defect analysis for large-scale photovoltaic farms". *IEEE Transactions on Energy Conversion*, vol. 34, no. 1, pp. 520–529, 2018.

[19] B. Li, C. Delpha, D. Diallo and A. Migan-Dubois. "Application of Artificial Neural Networks to photovoltaic fault detection and diagnosis: A review". *Renewable and Sustainable Energy Reviews*, vol. 138, pp. 110512, 2021.

[20] S. Mehta, A. P. Azad, S. A. Chemmengath, V. Raykar and S. Kalyanaraman. "DeepSolarEye: Power Loss Prediction and Weakly Supervised Soiling Localization via Fully Convolutional Networks for Solar Panels". In *2018 IEEE Winter Conference on Applications of Computer Vision (WACV)*, pp. 333–342, 2018.

[21] A. L. C. Ottoni, R. M. de Amorim, M. S. Novo and D. B. Costa. "Tuning of data augmentation hyperparameters in deep learning to building construction image classification with small datasets". *International Journal of Machine Learning and Cybernetics*, vol. 14, no. 1, pp. 171–186, 2023.

[22] C. Shorten and T. M. Khoshgoftaar. "A survey on image data augmentation for deep learning". *Journal of big data*, vol. 6, no. 1, pp. 1–48, 2019.

[23] L. Perez and J. Wang. "The effectiveness of data augmentation in image classification using deep learning". *arXiv preprint arXiv:1712.04621*, 2017.

[24] H. S. Peinado, C. A. de Oliveira, A. L. C. Ottoni, R. R. S. de Melo, D. B. Costa and M. S. Novo. "Análise de técnicas de data augmentation para aperfeiçoamento da detecção de sistemas de guarda-corpo e rodapés em canteiros de obras com inteligência artificial". *Simpósio brasileiro de gestão e economia da construção*, vol. 13, pp. 1–10, 2023.

[25] P. Chen, S. Liu, H. Zhao and J. Jia. "Gridmask data augmentation". *arXiv preprint arXiv:2001.04086*, 2020.

[26] P. Rici, S. O. S. Santos and A. L. C. Ottoni. "Tuning of Data Augmentation Hyperparameters to COVID-19 Detection in X-Ray Images with Deep Learning". *Journal of the Brazilian Society on Computational Intelligence (SBIC)*, vol. 20, no. 2, pp. 5–20, 2020.

[27] A. Mikołajczyk and M. Grochowski. "Data augmentation for improving deep learning in image classification problem". In *2018 international interdisciplinary PhD workshop (IIPhDW)*, pp. 117–122. IEEE, 2018.

[28] X. Ying. "An overview of overfitting and its solutions". In *Journal of physics: Conference series*, volume 1168, p. 022022. IOP Publishing, 2019.

[29] A. Bartler, L. Mauch, B. Yang, M. Reuter and L. Stoicescu. "Automated detection of solar cell defects with deep learning". In *2018 26th European signal processing conference (EUSIPCO)*, pp. 2035–2039. IEEE, 2018.

[30] M. Le, D. K. Nguyen, V.-D. Dao, N. H. Vu, H. H. T. Vu *et al.*. "Remote anomaly detection and classification of solar photovoltaic modules based on deep neural network". *Sustainable Energy Technologies and Assessments*, vol. 48, pp. 101545, 2021.

[31] L. Taylor and G. Nitschke. "Improving deep learning with generic data augmentation". In *2018 IEEE symposium series on computational intelligence (SSCI)*, pp. 1542–1547. IEEE, 2018.

[32] H. Sai. "Solar Panel dust detection". `https://www.kaggle.com/datasets/hemanthsai7/solar-panel-dust-detection/data`. Acesso em: 15 de dezembro de 2023.

[33] S. A. Ali. "Solar Panel Images Clean and Faulty Images". `https://www.kaggle.com/datasets/pythonafroz/solar-panel-images`. Acesso em: 15 de dezembro de 2023.

[34] S. Targ, D. Almeida and K. Lyman. "Resnet in Resnet: Generalizing Residual Architectures". *CoRR*, vol. abs/1603.08029, 2016.

[35] S. Targ, D. Almeida and K. Lyman. "Resnet in resnet: Generalizing residual architectures". *arXiv preprint arXiv:1603.08029*, 2016.

[36] K. He, X. Zhang, S. Ren and J. Sun. "Deep residual learning for image recognition". In *Proceedings of the IEEE conference on computer vision and pattern recognition*, pp. 770–778, 2016.

[37] D. Theckedath and R. Sedamkar. "Detecting affect states using VGG16, ResNet50 and SE-ResNet50 networks". *SN Computer Science*, vol. 1, no. 2, pp. 79, 2020.

[38] M. Elpeltagy and H. Sallam. "Automatic prediction of COVID- 19 from chest images using modified ResNet50". *Multimedia tools and applications*, vol. 80, no. 17, pp. 26451–26463, 2021.

[39] F. Pedregosa, G. Varoquaux, A. Gramfort, V. Michel, B. Thirion, O. Grisel, M. Blondel, P. Prettenhofer, R. Weiss, V. Dubourg, J. Vanderplas, A. Passos, D. Cournapeau, M. Brucher, M. Perrot and E. Duchesnay. "Scikit-learn: Machine Learning in Python". *Journal of Machine Learning Research*, vol. 12, pp. 2825–2830, 2011.

[40] J. Wang, B. Zhao and X. Yao. "PV abnormal shading detection based on convolutional neural network". In *2020 Chinese Control And Decision Conference (CCDC)*, pp. 1580–1583. IEEE, 2020.

[41] H. Chen, Y. Pang, Q. Hu and K. Liu. "Solar cell surface defect inspection based on multispectral convolutional neural network". *Journal of Intelligent Manufacturing*, vol. 31, no. 2, pp. 453–468, 2020.

[42] B. Su, H. Chen and Z. Zhou. "BAF-detector: An efficient CNN-based detector for photovoltaic cell defect detection". *IEEE Transactions on Industrial Electronics*, vol. 69, no. 3, pp. 3161–3171, 2021.

[43] S. Ding, Q. Yang, X. Li, W. Yan and W. Ruan. "Transfer Learning based Photovoltaic Module Defect Diagnosis using Aerial Images". In *2018 International Conference on Power System Technology (POWERCON)*, pp. 4245–4250, 2018.